

Estimation of dust related ice nucleating particles in the atmosphere

Comparison of profiling and in-situ measurements

Moritz Haorig^{1*}, Albert Ansmann¹, Adrian Walser², Holger Baars¹, Claudia Urbanneck¹, Bernadett Weinzierl², Manuel Schöberl², Maximilian Dollner², Rodanthi Mamouri³, and Dietrich Althausen¹

¹Leibniz Institute for Tropospheric Research (TROPOS), Leipzig, Germany

²Faculty of Physics, University of Vienna, Vienna, Austria

³Cyprus University of Technology, Dep. of Civil Engineering and Geomatics, Limassol, Cyprus

Abstract. Vertical profiles of number concentrations of dust particles relevant for ice nucleation in clouds are derived from lidar measurements. The results are compared to coincidental airborne in-situ measurements of particle number and surface area concentrations in the dust layer. The observations were performed in long-range transported Saharan dust at Barbados and Asian dust at Cyprus. The Asian dust data analysis is ongoing. A comparison of Asian and Saharan dust will be given at the conference. Concentrations of ice nucleating particles in the order of 10 to 1000 per cm^{-3} in the dust layer are derived for a temperature of -25°C at Barbados. The method can be used to continuously monitor the concentration of ice nucleating dust particles vertically resolved from lidar measurements.

1 Introduction

Dust particles not only influence visibility and health, but also cloud properties. In the formation of clouds they serve as cloud condensation nuclei (CCN). Their ability to partly serve as ice nucleating particles (INP) influences ice formation and precipitation and thus the hydrological cycle as a whole. The ice crystal number concentration in clouds is highly variable in time and space influencing strongly the cloud radiative properties. To improve our understanding of the interaction between dust particles and cloud properties and therefore precipitation processes, vertical profiles of dust related INP would be beneficial.

Laboratory studies intensively investigated the ability of dust particles to serve as INP [1, 2]. Number concentration and surface area concentration related parametrizations were found for the immersion freezing mode [3–6]. In atmospheric measurements, the particle extinction derived from the lidar can be used to derive a vertical profile of the number concentration of large particles ($D > 500$ nm) and the surface area concentration [7]. Using the laboratory parametrization a vertical profile of the ice nucleating particles can be derived. The parametrization strongly depends on temperature.

Aircraft in-situ measurements offer the opportunity to validate the derived profiles of number concentration and surface area concentration. We present results from two campaigns, the Saharan Aerosol Long-range Transport and Aerosol–Cloud–interaction Experiment (SALTRACE) at Barbados [8] and A-Life (Absorbing aerosol layers in a changing climate: aging, lifetime and dynamics) at Cyprus. In both campaigns the Falcon aircraft performed

in-situ measurements in the dust layers close to the lidar site. Depending on source region, e.g. Sahara versus Central Asia, mineral dust has different mineralogical properties [1], resulting in slightly different optical properties [9]. This contribution will discuss the differences in INP concentrations found for Saharan and Asian dust. In this abstract only one example from Barbados will be presented.

2 Instrumentation

A polarization lidar is necessary to estimate the vertical profile of dust particles which are large enough ($D > 500$ nm, according to the parametrization by DeMott [3, 4]) to serve as ice nucleating particles at a certain temperature. The polarization technique is used to separate the aerosol types and to identify the dust component [7]. The polarization lidars used at Barbados and Cyprus are described in [10] and [11], respectively.

Two optical particle counters (Grimm Sky 1.129, size range 0.25–2.5 μm) and two condensation particle counters (CPC, size range 0.005–2.5 μm) were used inside the research aircraft Falcon (Deutsches Luft- und Raumfahrtzentrum, DLR). On the wing of the aircraft a Cloud and Aerosol Spectrometer with Depolarization (CAS-DPOL, size range 0.5–50 μm) and an Ultra-High Sensitivity Aerosol Spectrometer-Airborne (UHSAS-A, size range 0.06–1 μm) were used. A detailed description of the retrieval of aerosol size distributions can be found in [12].

3 Results

An extended Saharan dust layer reached Barbados (13°N , 59°W) on 10 July 2013 [10]. The layer reached 5 km

*Corresponding author, haorig@tropos.de

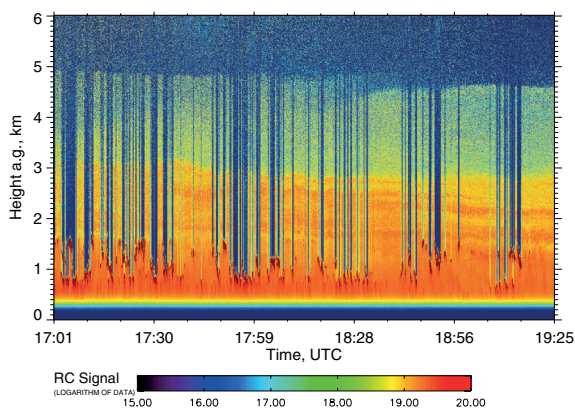


Figure 1. Saharan dust plume measured with lidar at Barbados, 10 July 2013, 13:01–15:25 local time. The lidar beam is extinguished in the cumulus clouds which are located between 0.7 and 1.5 km height (shown in dark red, no signal above a cloud). A dense Saharan dust layer (approx. 1.8 – 3 km height) is topped by a less dense Saharan dust layer (approx. 3 – 5 km). The range corrected signal at 532 nm (cross polarized) is shown in this time-height plot.

in altitude as can be seen in Fig. 1. At daytime a lot of cumulus clouds between 700 and 1500 m height are present. Only the cloud free profiles are used for the lidar analysis. The Falcon aircraft was flying at the east coast of Barbados just 30 km upwind of the lidar station.

The profile of the particle backscatter coefficient (Fig. 2a) will be separated in dust and non-dust components (marine or continental aerosol) by using the particle linear depolarization ratio. The high depolarization ratio (0.3) above 1.8 km height clearly indicates the dominance of dust in the Saharan air layer. The dust-related backscatter coefficient is converted to a dust-related extinction coefficient by using an extinction-to-backscatter ratio (lidar ratio) typical for Saharan dust of 55 sr. The extinction coefficient can be directly converted to a number concentration of particles larger than 250 nm in radius [7], shown in Fig. 2b. With a similar approach the dust-related extinction can be converted to surface area concentration (Fig. 2c) [7].

The number concentration of particles larger than 250 nm in radius can be compared to the optical particle counters operated aboard the Falcon aircraft. The in-situ measured number concentrations for ambient conditions in this case are slightly lower, but agree within the uncertainties (Fig. 2b).

The surface area concentration has to be calculated from the in-situ measured and parametrized particle number concentrations. A few coarse mode particles dominate the overall surface area. The derived vertical profiles of number concentration ($r > 250$ nm) and the surface area concentration can be confirmed within the uncertainties by the airborne in-situ measurements.

In a next step, the parametrization by DeMott [3, 4] for the particle number concentration with radius > 250 nm

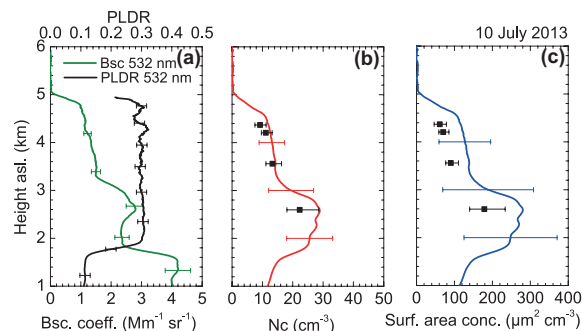


Figure 2. From optical to microphysical properties. The lines show the lidar measurement (13:01–15:25 LT, cloud free profiles) and the black dots are Falcon measurements (12:30–14:32 LT, ambient conditions) on 10 July 2013. Vertical profiles of (a) the particle backscatter coefficient (Bsc. coeff.) and the particle linear depolarization ratio (PLDR) at 532 nm, (b) the number concentration (N_c) of particles with radius > 250 nm and (c) the surface area concentration.

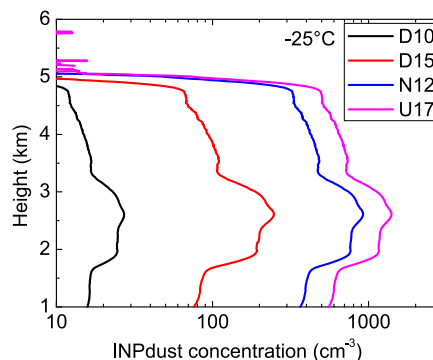


Figure 3. Number concentration of dust related ice nucleating particles at -25°C at Barbados (10 July 2013, 13:01–15:25 LT). The parametrizations are taken from DeMott [3, 4] (D10, D15), Niemand [5] (N12), and Ullrich [6] (U17).

and from Niemand [5] and Ullrich [6] for the surface area concentration can be used to derive the concentration of INP from immersion freezing. Figure 3 presents the results for a given temperature of -25°C . The ambient temperature in the dust layer was above 0°C inhibiting ice formation. The concentration of INP (at -25°C) will become atmospherically relevant in case the dust is lifted to higher altitudes by deep convection or in case of further long-range transport to higher latitudes. In both cases temperatures of -25°C are realistic.

At -25°C , there will be between 10 and 1000 (per cm^{-3}) ice nucleating particles among the dust. This number will increase significantly for lower temperatures. The parametrization by DeMott (D10) [3] covers all particles larger than 250 nm in radius and leads to lower INP concentrations around 10 per cm^{-3} (at -25°C). Whereas the parametrization by DeMott (D15) [4] was explicitly made for dust particles and leads to higher INP concentrations. The surface area based parametrizations by Niemand (N12) [5] and Ullrich (U17) [6] lead to 5 till 8 times

higher INP concentrations than the number concentration based parametrization for dust by DeMott (D15). The laboratory based parametrization introduces a large uncertainty (factor 3–10), but it gives an idea about the orders of magnitude to expect the INP.

4 Conclusion

The method to derive INP concentrations from polarization lidar measurements presented by Mamouri and Ansmann, 2016, [7] showed for the presented case study good agreement for the basic quantities of particle number concentration (for $r > 250$ nm) and surface area concentration compared to coincidental airborne in-situ observations at Barbados. The quality of the derived INP concentration depends on the parametrizations from laboratory measurements. The order of magnitude for dust INP concentrations is already sufficient to improve the predictions and to study the relations of dust particles and ice formation in clouds. Naturally, the INP concentrations vary within orders of magnitude on a small scale. In a next step, these INP parametrizations will be compared to the number concentration of ice crystals in an ice cloud, as will be shown in Ansmann's contribution to CADUC. Here, only an example for Saharan dust is shown, but more comparisons of aircraft and lidar observations for Asian dust in Cyprus will follow at CADUC. Once we have confidence in the INP parameterizations from polarization lidar, it can be used to monitor INP concentrations from continuous lidar observations from ground (AD-Net, EARLINET, PollyNET) [13–15] and space (CALIPSO, EarthCARE).

References

- [1] Murray, B. J., D. O'Sullivan, J. D. Atkinson, and M. E. Webb, *Chem. Soc. Rev.*, **41**, 6519–6554 (2012).
- [2] Hoose, C., and O. Möhler, *Atmos. Chem. Phys.*, **12**, 9817–9854 (2012).
- [3] DeMott, P. J., Prenni, A. J., Liu, X., Kreidenweis, S. M., Petters, M. D., Twohy, C. H., Richardson, M. S., Eidhammer, T., and Rogers, D. C.m, *P. Natl. Acad. Sci. USA*, **107**, 11217–11222 (2010).
- [4] DeMott, P. J., Prenni, A. J., McMeeking, G. R., Sullivan, R. C., Petters, M. D., Tobo, Y., Niemand, M., Möhler, O., Snider, J. R., Wang, Z., and Kreidenweis, S. M., *Atmos. Chem. Phys.*, **15**, 393–409 (2015).
- [5] Niemand, M., Möhler, O., Vogel, B., Vogel, H., Hoose, C., Connolly, P., Klein, H., Bingemer, H., DeMott, P., Skrotzki, J., and Leisner, T., *J. Atmos. Sci.*, **69**, 3077–3092 (2012).
- [6] Ullrich, R., C. Hoose, O. Möhler, M. Niemand, R. Wagner, K. Höhler, N. Hiranuma, H. Saathoff, and T. Leisner, *J. Atmos. Sci.*, **74**, 699–717 (2017).
- [7] Mamouri, R.-E. and Ansmann, A., *Atmos. Chem. Phys.*, **16**, 5905–5931 (2016).
- [8] Weinzierl, B., Ansmann, A., Prospero, J. M., Althausen, D., Benker, N., Chouza, F., Dollner, M., Farrell, D., Fomba, W. K., Freudenthaler, V., Gasteiger, J., Groß, S., Haarig, M., Heinold, B., Kandler, K., Kristensen, T. B., Mayol-Bracero, O. L., Müller, T., Reitebuch, O., Sauer, D., Schäfler, A., Schepanski, K., Spanu, A., Tegen, I., Toledano, C., and Walser, A., *B. Am. Meteorol. Soc.*, **98**, 1427–1451 (2017).
- [9] Hofer, J., Althausen, D., Abdullaev, S. F., Makhmudov, A. N., Nazarov, B. I., Schettler, G., Engelmann, R., Baars, H., Fomba, K. W., Müller, K., Heinold, B., Kandler, K., and Ansmann, A., *Atmos. Chem. Phys.*, **17**, 14559–14577 (2017).
- [10] Haarig, M., Ansmann, A., Althausen, D., Klepel, A., Groß, S., Freudenthaler, V., Toledano, C., Mamouri, R.-E., Farrell, D. A., Prescod, D. A., Marinou, E., Burton, S. P., Gasteiger, J., Engelmann, R., and Baars, H.: , *Atmos. Chem. Phys.*, **17**, 10767–10794 (2017).
- [11] Engelmann, R., Kanitz, T., Baars, H., Heese, B., Althausen, D., Skupin, A., Wandinger, U., Komppula, M., Stachlewska, I. S., Amiridis, V., Marinou, E., Mattis, I., Linné, H., Ansmann, A., *Atmos. Meas. Tech.*, **9**, 1767–1784 (2016).
- [12] Walser, A., Sauer, D., Spanu, A., Gasteiger, J., and Weinzierl, B., *Atmos. Meas. Tech.*, **10**, 4341–4361 (2017).
- [13] Nishizawa, T., Sugimoto, N., Matsui, I., Shimizu, A., Hara, Y., Itsushi, U., Yasunaga, K., Kudo, R., and Kim, S.-W., *JQSRT*, **188**, 79 – 93 (2017).
- [14] Pappalardo, G., Amodeo, A., Apituley, A., Comeron, A., Freudenthaler, V., Linné, H., Ansmann, A., Bösenberg, J., D'Amico, G., Mattis, I., Mona, L., Wandinger, U., Amiridis, V., Alados-Arboledas, L., Nicolae, D., and Wiegner, M., *Atmos. Meas. Tech.*, **7**, 2389–2409 (2014).
- [15] Baars, H., Kanitz, T., Engelmann, R., Althausen, D., Heese, B., Komppula, M., Preißler, J., Tesche, M., Ansmann, A., Wandinger, U., Lim, J.-H., Ahn, J. Y., Stachlewska, I. S., Amiridis, V., Marinou, E., Seifert, P., Hofer, J., Skupin, A., Schneider, F., Bohlmann, S., Foth, A., Bley, S., Pfuller, A., Giannakaki, E., Lihavainen, H., Viisanen, Y., Hooda, R. K., Pereira, S. N., Bortoli, D., Wagner, F., Mattis, I., Janicka, L., Markowicz, K. M., Achtert, P., Artaxo, P., Pauliquevis, T., Souza, R. A. F., Sharma, V. P., van Zyl, P. G., Beukes, J. P., Sun, J., Rohwer, E. G., Deng, R., Mamouri, R.-E., and Zamorano, F., *Atmos. Chem. Phys.*, **16**, 5111–5137 (2016).